Case Studies in Thermal Engineering 49 (2023) 103170

Contents lists available at ScienceDirect

Case Studies in Thermal Engineering

journal homepage: www.elsevier.com/locate/csite

Optimization and Modelling of EGR rate and MIS for POME fuelled CRDI diesel engine

S.A. Alur [a], M.M. Shivashimpi [b,**], K.M. Akkoli [b], J. Samson Isaac [c], N.R. Banapurmath [d], D. Sakthivel [e], Yogesh Diliprao Sonawane [f], Saiful Islam [g], Prabhakar Sharma [h], Mohammad Amir Khan [i], Abdul Razak [j,*]

[a] Department of Mechanical Engineering, S.G. Balekundri Institute of Technology, Belagavi, Karnataka, 590010, India
[b] Department of Mechanical Engineering, Hirasugar Institute of Technology, Nidasoshi, Karnataka, 591236, India
[c] Department of Biomedical Engineering, Karunya Institute of Technology and Sciences, Coimbatore, 641114, India
[d] School of Mechanical Engineering, KLE Technological University, Hubballi, Karnataka, India
[e] Department of Mechanical Engineering, St. Joseph's College of Engineering, Chennai-119, India
[f] Shri Vile Parle Kelavani Mandal's Institute of Technology, Dhule, Maharashtra, India
[g] Civil Engineering Department, College of Engineering, King Khalid University, Abha, 61421, Saudi Arabia
[h] Department of Mechanical Engineering, Delhi Skill and Entrepreneurship University, Delhi, 110089, India
[i] Department of Civil Engineering, Galgotia College of Engineering, Greater Noida, 201310, India
[j] Department of Mechanical Engineering, P. A. College of Engineering (Affiliated to Visvesvaraya Technological University, Belagavi), Mangaluru, 574153, India

ARTICLE INFO

Handling Editor: Huihe Qiu

Keywords:
Palm oil methyl ester
CRDI
EGR
Multiple injection strategies
Oxide of nitrogen
Performance

ABSTRACT

In the present research work an optimisation stuy of the Exhaust gas recirculation (EGR) rate for MIS adopted POME fueled CRDI Diesel Engine fitted with TRCC was carried out. The engine was operated with injection parameters such as 900 bar, 7 holes and 10° BTDC which have been optimized for better performance and lower emissions from our previous study. The experiments were carried out by employing an RSM-based D-optimal design, and the relationship between input and output was determined using an ANOVA. Using RSM-ANOVA, mathematical models were built for each result, and the predicted and actual outcomes were compared. With an R^2 value greater than 99.34%, the prediction models were discovered to have a strong prediction efficiency. The desirability approach-based optimisation was used to determine the ideal engine operating parameters. EGR rate was varied from 0% to 20% and an MIS of 40 + 20+40 has been adopted for the engine. An EGR rate of 10% is optimized from the viewpoint of NO_x reduction and penalty in power output which results in a decrease in brake thermal efficiency by 2.90%, peak pressure by 4.8%, heat release rate by 8.8% and oxides of nitrogen (NO_x) by 1.35%. A drastic increase in emissions such as carbon monoxide by 5.8%, unburnt hydrocarbon by 13.3% and smoke by 20.6% was also observed. Both the ANN and RSM models correctly fit the experimental data, producing R^2 values that ranged from 95.5% to 98.5%, respectively. The findings show that RSM and ANN are both highly accurate modelling approaches. Additionally, as compared to RSM, the

* Corresponding author.
** Corresponding author.
E-mail addresses: saalur@gmail.com (S.A. Alur), mmshivashimpi.mech@hsit.ac.in (M.M. Shivashimpi), kmakkoli.mech@hsit.ac.in (K.M. Akkoli), Samsonisaac@karunya.edu (J. Samson Isaac), nrbanapurmath@gmail.com (N.R. Banapurmath), devarajusakthivel@gmail.com (D. Sakthivel), yogeshsonaw@gmail.com (Y.D. Sonawane), sfakrul@kku.edu.sa (S. Islam), amirmdamu@gmail.com (M. Amir Khan), abdulkaladgi@gmail.com (A. Razak).

https://doi.org/10.1016/j.csite.2023.103170
Received 25 April 2023; Received in revised form 31 May 2023; Accepted 7 June 2023
Available online 10 June 2023

ANN model's predictive accuracy was marginally better. This research could have a wide range of applications in CI engine-powered transportation systems.

Nomenclature

BP	Brake power
BSFC	Brake specific fuel consumption
bTDC	Before top dead centre
CCC	Cylindrical combustion chamber
CD	Combustion duration
CO	Carbon monoxide
CR	Compression ratio
COME	Cotton oil methyl ester
CRDI	Common rail direct injection
DOE	Design of experiment
ECU	Electronic control unit
EGT	Exhaust gas temperature
HCC	Hemispherical combustion chamber
HOME	Hongeoil methyl ester
HnOME	Honne oil methyl ester
HRR	Heat release rate
IT	Injection timing
IOP	Injection opening pressure
ID	Ignition delay
JOME	Jatropha oil methyl ester
MIS	Multiple injection strategies
NIG	Nozzle injector geometry
NO_x	Oxides of Nitrogen
POME	Palm oil methyl ester
PP	Peak pressure
SCC	Shallow depth combustion chamber
SIS	Single injection strategy
TCC	Toroidal combustion chamber
TRCC	Toroidal reentrant combustion chamber
UBHC	Unburnt hydrocarbon

1. Introduction

Diesel engine discharge characteristics are primarily influenced by fuel qualities, combustion chamber type, and injection settings [1]. NO_x is the major pollutant from Diesel engines apart from other pollutants like particulate matter (PM), unburned hydrocarbons & Carbon monoxide. Peak temperatures attained during the combustion process favour the formation of NO_x.NO_x emission can not be removed from the exhaust gases by the pretreatment process. Controlling the temperatures of the air fuel mixture is the only method to reduce NO_x [1]. Higher level of NO_x emission cause respiratory problems, and forms ground-level ozone which is a major component of smog. NO_x results in acid rain which causes the deterioration of the materials and buildings. NO_x emission also results in global warming.

Biodiesel fuel has more O_2 content as compared to diesel and results in a still higher level of NO_x emissions. Reduction in NO_x emission can be achieved by injecting the water, emulsion technology, retarding the IT, EGR and combining the EGR with other methods [2]. Experiments conducted to investigate the impact of blend strength on NO_x emission emitted by CRDI engines fueled with n-Butanol Blends disclosed that the use of n-butanol blends has to be restricted to NB20 because of the drastic increase in NO_x emissions for blend strengths beyond NB20 [3]. EGR consists of recirculating a certain portion of exhaust gases into the engine thereby enhancing the thermal capacity of the in-cylinder air mixture. This will cause a decrease in the combustion chamber temperature and hence NO_x tend to minimize from the engine. But CO_2 content in the recirculated gases will reduce the O_2 concentration of the in-cylinder fuel-air mixture resulting in incomplete combustion. This decreases the useful work output and the unburnt fuel amount increases [4]. The hot exhaust gas recirculation of diesel fuels has to be restricted up to 15% to single-cylinder, four-stroke engines due to adverse effects on engine performance and SFC [5]. The engine using bran oil methyl ester gave reduced NO_x emission by retardation of IT, EGR and IOP [6]. The diesel engine operated with biomass fuel (1-hexanol and its mixtures) with diesel fuel gave elevated combustion properties such as ID, PP, and HRR at 25° bTDC and 30% of EGR [7]. At the same optimized conditions, emissions properties such as smoke could be reduced by 35.9% with a penalty of 3% NO_x. Engine exhaust emission results showed that mixed fuel diminishes the NOx emission by 4.96% and smoke emission by 11.0% and enhance specific CO2 by 3.4% for SMB20 blend at full load condition when engine is operated at advance injection timing and higher injection pressure [8].

CRDI can inject a very high-pressure fuel directly into the engine manifold through electronically controlled multiple injectors at any desired pressure at any time. Greater injection pressure produces finer fuel atomization and improves air-fuel mixing. *MIS* consists of splitting the fuel injection into 2 to 3 injections spread over a wider time instead of injecting all the fuel in a stipulated time. This reduces the attainment of peak combustion chamber temperature in the cylinder.CRDI engine combined with multiple injection strategies (MIS) will improve performance, attains fuel economy and reduces emissions, particularly NO_x emissions. Biodiesel prepared from Simaroubaoil [9] and Mahua oil [8] shows improved performance and reduced emissions when operated at higher pressures in CRDI diesel engines. Improved performance and drop in emissions are achieved when the CRDI biodiesel-fueled diesel engine is operated at higher pressure with the modified combustion chamber (TRCC shape) and optimized injection parameters [10]. The plastic oil biodiesel blend B30 in CRDI engine gives a drop in NO_x emissions with an increase in blend strength but at the cost of BTE [11]. However, the Karanja biodiesel blend B20 in the CRDI engine gives a drop in emissions with improved performance [12]. The particulate matter of smaller size was noticed in the CRDI engine operated at advanced IOP and retardation in IT [13]. The modified CRDI engine using POME fuel gave a higher performance for 7 holes *NIG* as compared to 6 holes *NIG* at optimized injection pressure and injection timing [14]. Tung oil blended diesel fuel gave improved combustion characteristics in the CRDI engine as contrasted to diesel [15]. Karanja biodiesel in the CRDI engine give improved performance as contrasted to diesel at −21° CA and 1000 bar *IOP* [16].

The pilot injection consists of injecting a less quantity of diesel fuel before the main injection. Pilot injection reduces the formation of NOx. NOx reduction techniques such as varying the fuel injection timing, and dilution of combustion gases by EGR are compared with the split injection strategy (25/75 and 75/25) by using a computational model and it is found that pilot injection of 25% of the main injection can reduce NO emissions significantly without much penalty on the brake thermal efficiency [17]. The rate of heat release was found to be lower while the fuel consumption was higher for a 100 KW Diesel engine adopted with multiple injection strategies as compared with the single pilot injection [18]. Low-temperature combustion can reduce NOx but is found to increase noise, CO and HC emissions [19]. Distribution of fuel among the different pulses in a multiple injection fuel system was used to control emissions and noise. The increase in the amount of fuel injected in the first pulse was used to reduce the unburnt emissions and the increase of fuel amount in the third pulse was found to reduce the noise [20].

Mahau oil methyl ester blend B5 gave a marginal penalty of BTE and drop in emissions as contrasted with standard diesel fuel when the engine was adopted with *MIS* techniques at 500 bar *IOP* [21]. The biodiesel-powered CRDI diesel engine performed better with triple injection strategies as compared to double injection strategies. The NO_x was reduced by 40.8% and 50%, meanwhile, smoke was reduced by 10% and 16.6% for double and triple strategies respectively [22]. The experiments conducted show that *MIS* with optimized pilot injection strategies can reduce the fuel consumed along with the emissions. The experimental results indicated that the optimized multi parameters such as 60% *EGR*, 90 MPa *IOP*, 0° *CA IT* and 10° aTDC pilot injection yielded lesser emission [23]. The modified CRDI diesel engine powered by POME gave an improved performance and reduced emissions except for NO_x at the combined effect of 900 bar, 10° bTDC, 7 *NIG*, 40 + 20+40 *MIS* combination, and TRCC shape [24]. Optimum parameters for better performance and emission features of biodiesel blends were discussed using various methods like Design of experiment method [25–33].

Multiple injection strategies can be used to lessen the peak temperature in the cylinder. MIS along with EGR is an effective method to reduce NO_x.Common Rail Direct Injection System (CRDI) along with EGR and MIS can be a promising strategy to improve performance and lower emissions including NO_x. The very minimal amount of study has been done using a customized combustion chamber design, NIG, IOP, IT, MIS, and EGR in a CRDI engine that is running on POME biodiesel fuel. Consequently, the goal of our present experiment is to optimize the EGR rate for POME with fixed parameters such as 10° bTDC, 900 bar *IOP*, 7 holes *NIG* and 40 + 20+40 *MIS* with TRCC shape. The main aim of this work is the reduction of emissions particularly NO_x with no compromise on performance and specific fuel consumption.

Table 1
Properties of POME [36]

Properties	Diesel	POME
Density (kg/m^3)	839	880
Energy density (KJ/kg)	43,010	38,400
Viscosity at 40 °C(CST)	2.44	3.94
Flash Point (°C)	74.8	160
Cetane Number	46–56	58
Carbon Residue (%)	0.099	–
Pour point (°C)	−4.9	6.7
Cetane Number	46–56	5
Sulphur (%)	0.005	0.05
Moisture (vol. %)	0.02	0.05
Acid value(mg KOH/gm)	0.35	0.800
distillate (°C)	160 with a 90% range	360 with a 97% range

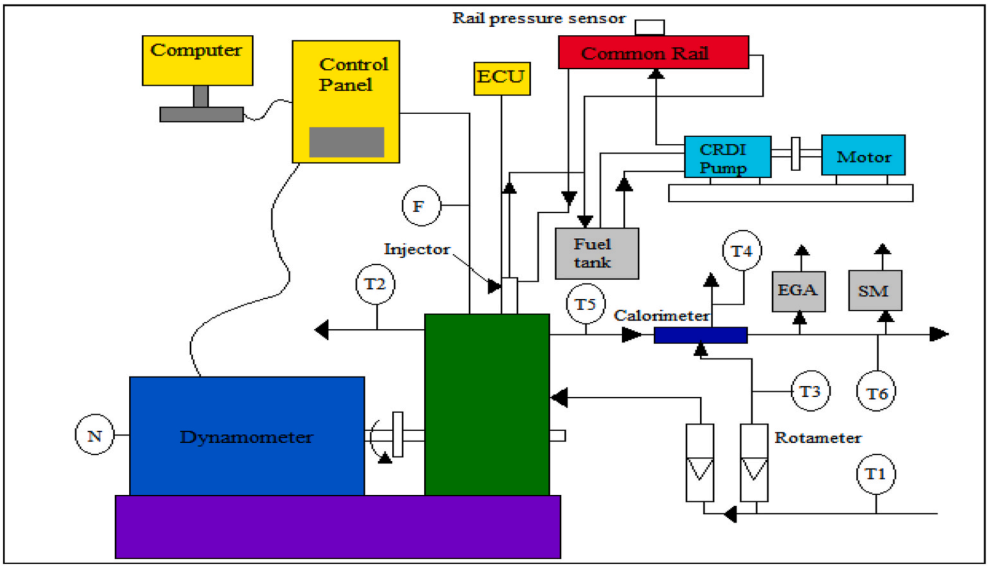

Fig. 1a. Schematic diagram of the experimental set-up of CI engine test rig with CRDI [42]
T1, T3 - Intake water temperature. T2 - Outlet engine jacket water temperature.T4 - Outlet Calorimeter water temperature T5 - Exhaust gas temperature before

Table 2
Specifications of the CI engine [42]

Parameter	Specification
Type	TV 1 (Kirloskar)
Software used	Engine soft
Nozzle opening pressure	220–225 bar
Governor type	Centrifugal type
Number of cylinders	01
Number of strokes	04
Fuel	H.S. Diesel
Rated power	5200 W (7 HP at 1500 rpm)
Bore	87.5 mm
Stroke length	110 mm
Compression ratio	17.5:1
Eddy current Dynamometer	
Model	AG-10
Type	Eddy current
Maximum	7500 W (at 1500–3000 RPM)
Fluid used	Water
Dynamometer arm length	0.180 m
Fuel measurement unit- range	0–50 ml

1.1. Objectives

1. To reduce the NO_x emissions of Palm biodiesel fueled engines without having to compromise more on engine performance.
2. To improve the combustion of fuel through finer atomization of the fuel and achieve low-temperature combustion conditions by using the CRDI fuel injection system with multiple injection strategies to control both the NO_x emissions and soot simultaneously
3. Overall the research work aims to improve the thermal efficiency of Palm biodiesel fueled engine by utilising the optimum combination of engine parameters.

2. Materials and methodology

The details of POME Biodiesel properties, experimental methodology, uncertainty analysis and design of the experiment are discussed in the following section.

2.1. Palm oil methyl ester properties

Palm is one of the highest oils produced in many perennial plants. This Palm oil is considered golden Palm due to its excessive compliance. In India, a Palm tree is grown on an area of approximately 50,000 ha under irrigation conditions and provides an excellent

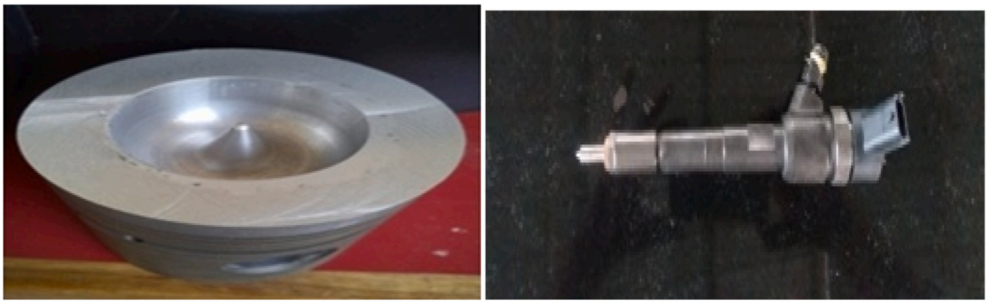

Fig. 1b. The CRDI injector and toroidal reentrant combustion chamber shape [36].

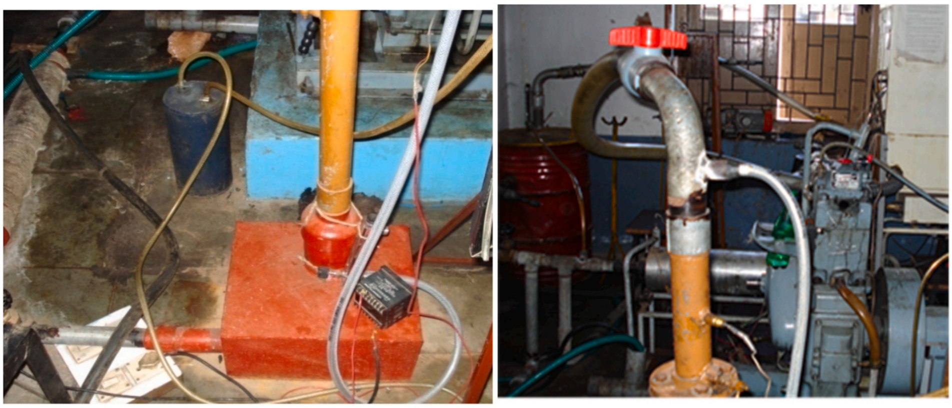

Fig. 1c. The details of exhaust gas recirculation [41].

substitute for oil imports. Palm trees can grow on a nominal plantation area compared to other trees. Plenty of full resources are available for the growth of Palm trees with the elevated production facility. Nearly 1/3rd of the total VO production can be expected from Palm trees alone. Only 10% of Palm oil is extractable as edible oil while the remaining 90% of the oil is disposed of as waste from the refinery oil industry. and thus, provides a potential source for the production of BDF [34,35]. The properties of Palm BDF have been compared with those of standard mineral DF as in Table 1. The viscosity of POME oil is 3.94 as compared to the viscosity of diesel which is 2.44. Palm BDF has a high Cetane number and this ensures that the DF engine powered by Palm BDF runs with less noise. The oxygen content of POME is 10.8.

The potential exists in India for 40–50 lakh tonnes of palm oil from 10.36 lakh hector potential area. The major o Palm oil-producing states in India are Andra Pradesh, Karnataka, Assam, Kerala, Gujrat, Gao, Tamilnadu, Maharashtra, Tripura, West Bengal, and some other places of Andaman. India has consistently increased its Palm oil production over the last five years from – 191,510 tonnes in 2014-15 to 278,922 tonnes in 2018-19 – an increase of about 45%. The total Palm oil potential area in India is about 1.93 million hectares spread across 19 states but the actual coverage is about 349,000 ha (up to October 2019) in 16 states. Of that, the approximate fruiting area is 135,000 ha in eight states. Andhra Pradesh (83.5%) along with Telangana accounts for about 97% of India's 278,000 tonnes of crude palm oil production. According to the government of India, six northeastern states – Mizoram,

Table 3
Uncertainty and accuracy levels of calculated engine parameters.

Parameters	Accuracy (±)	Uncertainty (%)
CO emission (%)	± 0.01	±0.3
NO_x emission (ppm)	± 10 ppm	±0.35
HC emission (ppm)	± 10 ppm	±0.38
EGT (°C)	± 1	±0.45
Smoke level (HSU)	± 1	±0.32
BTE(%)	–	±0.5
BSFC (%)	–	±0.40
HRR (J/°CA)	–	±0.15

Arunachal Pradesh, Meghalaya, Tripura, Nagaland, and Assam together have a potential area of 218,000 ha for palm oil crops but less than 20% of this was under plantation till 2019.

The MIS and fuel properties are correlated with the viscosity of the fuel [36–42]. The fuel injection at different injection intervals associated with optimized injection pressure reduces the viscosity of POME and further improves air-fuel mixing. This, in turn, facilitates complete combustion of the fuel during post-injection of POME.

2.2. Experimental setup and methodology

The experimental setup has been shown in Fig. 1a. The main specifications of the engine are enumerated in Table 2. A piezoelectric transducer was used for the measurement of inline cylinder pressure. The Hartridge smoke meter and five-gas analyzers (A DELTA 1600 S) are used for the measurement of smoke opacity and emissions respectively. The experiment is conducted at a constant speed of 1500 r.p.m. Modifications made in the research engine are as follows. CRDI system has been developed in-house with a high-pressure injection facility being incorporated into the engine. CRDI system is controlled by an electronic control unit (ECU) facility. The ECU system is one of the electronic facilities attached to the CRDI biodiesel fueled diesel engine and its function is to control the fuel injection, timing, and oxygen quantity, with the help of sensors. The engine is powered by POME as an alternative fuel being injected with adopted multiple injection strategies (MIS) of 40-20-40 combination. Fuel injection is divided into pilot injection (40%) at 20^{o}BTDC, main injection (20%) at TDC) and post-injection (40%) at 5oATDC respectively. The fuel consumption rate varied with loads and pressures. At peak load, the injection rates of fuels varied from 10 mg/s to 25 mg/s when injection pressure was varied from 600 bar to 1000 bar.

The TRCC shape is developed keeping the same compression ratio of 17.5 as in the existing HCC shape and fabricated using a CNC machine. The existing HCC shape is replaced by the TRCC shape (shown in Fig. 1b) in the engine. Droplet size was measured in the range from 2 μm to 75 μm. Multi-hole nozzle having 7 holes is shown in Fig. 1b. The injection parameters optimized from our previous research work such as 7 holes NIG, 10° BTDC and 900 bar IOP have been adopted with the CRDI system. Two valves are provided to control the EGR rate. Exhaust gases are passed through a silica gel container before being redirected into the engine. Fig. 1c shows the arrangement for the EGR attachment. The parameters such as 10° bTDC, 900 bar IOP, 7 holes NIG, 40 + 20+40 MIS and TRCC shape have been kept constant throughout the experiments in the CRDI diesel engine. The exhaust Gas Recirculation (EGR) rate varies from 0% to 20% and experimental values are compared with those obtained using neat diesel fuel. As an increased EGR rate increases the percentage of carbon dioxide in the air-fuel mixture and at EGR rates beyond 20% more dilution results in an incomplete combustion process. The percentage of EGR is varied from 0% to 20% to avoid the higher BTE penalty from a diesel engine.EGR percentage is chosen such that the trade-off is done regarding smoke and NO_x emissions with acceptable engine performance.

Experiments are conducted to study the effect of EGR rate on the performance, emission and combustion characteristics of POME operated with an optimized MIS combination (40 + 20+40). The objective of the MIS technique is to inject the fuel over a wider time window to give enough time for the mixing of air with the fuel. Fuel injection is divided into pilot fuel injection, main injection, and post-injection with 40%, 20% and 40% of the fuel being injected respectively. EGR rate is varied from 0% to 20%. The experiments are carried out on a modified CRDI DF engine under optimized conditions of the engine such as IOP 900 bar, IT 10°bTDCand 7 holes NIG with TRCC shape at different loads. The experiment results are compared with the single injection strategy adopted for the DF. The detailed performance, combustion and emission properties of the engine are discussed.

The experiments were conducted at 20%, 40%, 80% and 100% loads. As the load increases BTE also increases for certain peak loads (80%) and later on, the performance of the engine is found to decrease. Hence the optimized 80% load was reported in the current research work.

2.3. Uncertainty analysis

Uncertainty analysis is the systematic and symmetric set of procedures followed for the calculation of errors in the experimental data recorded.

The overall uncertainty of the parameters of engine performance, emission, and combustion is calculated using Equation (1).

$$\mathbf{Overall Uncertainity} = \pm\sqrt{\text{Uncertainityof }\%\left(\text{BTE}^2+\text{BSFC}^2+\text{CO}^2+\text{NO}_{\text{X}}{}^2+\text{HC}^2+\text{smoke}^2+\text{HRR}^2+\text{EGT}^2\right)} \tag{1}$$

$$= \pm\sqrt{\text{Uncertainityof }\%\left(0.5^2+0.40^2+0.3^2+0.35^2+0.38^2+0.32^2+0.15^2+0.45^2\right)}$$

$$= \pm\mathbf{1.04}$$

Table 3 also illustrates the uncertainty and accuracy levels of calculated engine parameters.

The overall uncertainty for the measured parameters is ±1.04, which is within the permissible limit and in symmetry with previously reported studies.

2.4. DOE by RSM and D-optimal design

RSM is a statistical method for optimising processes, products, and systems. The employment of mathematical models to describe the link between one or more input variables (factors) and one or more output variables is involved (responses). The fundamental goal of RSM is to determine the ideal combination of parameters that results in the largest or smallest interest response. RSM does this through a series of tests or trials conducted under various combinations of factor levels. The outcomes of these tests are then utilised to

Table 4
Design matrix on the basis of d-optimal design.

Exp.Run No.	Load %	EGR %	BTE, %	EGT, C	CO, %Vol.	NOx, ppm	UHBC, ppm
15	20	0	16.55	150	0.04	147	12
11	30	5	20.11	181	0.062	189	16
13	100	20	27.58	454	0.18	928	58
14	80	0	31	357	0.12	811	30
10	60	20	26.38	235	0.154	525	32
8	20	10	15.79	138	0.064	141	16
1	20	20	14.72	125	0.144	135	20
16	100	7	29.02	465.5	0.167	940	52.5
5	100	20	27.58	454	0.18	928	58
3	80	0	31	357	0.12	811	30
6	60	12	27.9	248	0.126	541	27
7	50	4	25.93	233	0.092	388.5	21
4	100	7	29.03	465	0.167	940	52.5
12	20	20	14.72	125	0.144	135	20
9	80	15	29.5	341	0.137	792	36
2	20	0	16.55	150	0.04	147	12

build a mathematical model that depicts the link between the variables and the desired response(s). RSM's mathematical models can take various forms, including linear, quadratic, and higher-order polynomial equations. These models are created utilising statistical approaches such as regression analysis, ANOVA, and DOE. Any combination of factor values within the experimental range may be anticipated by the model after it has been constructed. The accuracy of the mathematical model and the quality of the experimental design determine the success of RSM in optimising processes, products, and systems. As a result, the selection of relevant factors, the range of factor values, the number of experiments, and the quality of data obtained throughout the experiments must all be carefully considered [26].

RSM is a sophisticated statistical approach that is widely used. Overall, RSM is a powerful statistical technique that is frequently utilised in engineering, chemistry, physics, and biology. It enables academics and practitioners to optimise processes and systems by determining the ideal mix of parameters that results in the best response (s).

RSM is a strong engine optimisation and modelling tool. RSM is used in the optimisation process to determine the ideal combination of engine operating parameters (i.e., factors) that result in optimal engine performance (i.e., response). For example, the goal could be to maximise engine power output, improve fuel efficiency, or reduce engine pollutants. To optimise the engine, a series of tests are designed utilising RSM to measure the engine's performance under various operating situations. The data obtained is then utilised to build a mathematical model that defines the connection between the input constraints and engine performance. The model can forecast engine performance for every combination of input parameters and determine the optimal parameter values that result in optimal engine performance. RSM is used in engine modelling to create mathematical models that characterise the engine's behaviour under various operating situations. These models can be used to mimic engine performance and study the effects of various operating settings on engine behaviour. RSM can, for example, be used to simulate the combustion process in an engine, which involves the interplay of numerous physical and chemical processes. The generated model can then be utilised to increase engine performance and reduce emissions by optimising the combustion process.

There are several experimental designs in RSM that can be utilised to generate the data required to develop a response surface model. Central Composite Design (CCD), Box-Behnken Design (BBD), and D-Optimal Design are three regularly utilised designs. A CCD design consists of a set of factorial points at the experimental region's corners, a set of axial points that extend beyond the corners, and

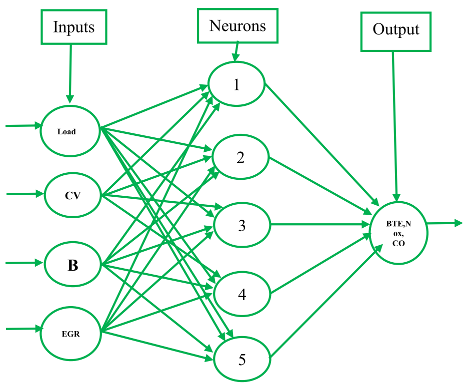

CV-Calorific value (KJ/Kg), B-Blends, BTE-Brake thermal Efficiency, NOx-Nitrogen oxide, Co-Carbon monoxide

Fig. 2. General ANN structure.

a set of centre points. The design is popular because it allows for the estimation of linear, quadratic, and interaction effects while also covering a large portion of the experimental region. BBD is a design that employs a similar set of factorial and axial points to CCD but lacks centre points. In terms of the number of experiments necessary to fit the model, the design is more efficient than CCD, although it may not provide as good coverage of the experimental region.

A D-Optimal Design is one that is optimised to reduce the variation of model parameter estimates. The optimal mix of factor levels is chosen in this design to minimise the uncertainty in model predictions. It is the most efficient design in terms of the number of tests necessary to fit the model, and it covers the experimental region well. D-Optimal Design is more inexpensive and efficient than CCD and BBD since it requires fewer tests to generate the same quantity of information. It also provides a more accurate estimate of the model parameters, lowering the danger of overfitting the model. D-Optimal Design, on the other hand, may be more difficult to apply because it requires specific tools and experience to develop the design and analyse the data [27]. Table 4 displays the planned array that was created using the D-optimal design.

2.5. Optimisation using desirability function

The desirability function is a technique used in response surface methodology (RSM) to simultaneously optimize numerous response variables. The goal of RSM is to determine the optimal levels of the input parameters that result in the best values of the response variables. When there are several response variables, it might be challenging to find a single set of input factor values that optimises all of the replies at the same time. The desirability function is a tool that combines several responses to provide a single overall response. It accomplishes this by giving each response variable a weight or relevance and merging them into a single score. The desirability score goes from 0 to 1, with 0 indicating that the response is not desirable and 1 indicating that the response is favourable. The desirability function allows for a more thorough approach to optimisation by taking into account several replies at the same time. It can be used to determine the greatest combination of factor levels that will generate the best overall response, even when the different responses have conflicting purposes. It also allows you to quantify the trade-offs between different replies and explain the results in a meaningful way. The desirability function in RSM is a powerful tool for optimising numerous response variables and determining the ideal combination of input component levels. It allows for a more complete approach to optimisation by converting various responses into a single overall response.

2.6. Modelling using artificial neural network(ANN)

A computer setup known as an artificial neural network is based on biological mechanisms, namely the way the human brain works. It consists of many linked processing units known as neurons that process data depending on their dynamic states in response to inputs. Neural networks use linked neurons to interpret the data that is supplied to them. The processing of the data is based on the strength of two adjusted neurons, or “weights,” which store the information that was learned during training, testing, and validation. By changing weights in relation to input trends, learning is achieved. The weights are changed to achieve adaptability to different circumstances. An ANN’s greatest strength is its capacity to anticipate the result of an unknown input. Neural networks are employed in decision support systems because forecasting is done by predicting the future based on prior experience. In engineering applications, neural networks are effective modelling and prediction tools.

An ANN model has three layers: the input layer, the hidden layer, and the output layer. (Fig. 2). The hidden layer initially links the output layer and input layer together [29]. The hidden layer’s bias and weights are then adjusted, and the gap between the actual and projected values is computed until the error is at a minimum [30]. The feed-forward with back propagation neural network model is used in the present study.

3. Results and discussion

Exhaust gas recirculation consists of reverting a certain portion of the gases from the exhaust pipe into the engine cylinder. It increases the thermal capacity of the air-fuel mixture in the cylinder and reduces the combustion temperature thus reducing NO_x.EGR will decrease the availability of oxygen required for combustion which results in incomplete combustion of the air-fuel mixture. Hence smoke, UBHC and CO have been found to increase with the increase in the EGR rate. The useful work output decreases and the unburnt fuel amount increases. Thus, brake thermal efficiency is found to decrease with an increase in the EGR rate. The effect of EGR on the performance, emission and combustion characteristics of POME-fueled diesel engines has been discussed in this section.

3.1. Impact of MIS and EGR rate on BTE

Table 5a reveals that the model has an F-value of 1022.45, indicating that it is statistically significant. This suggests that such a huge F-value is extremely rare (only a 0.01% chance) to arise owing to random noise in the data. Individual model terms (A, B, and A2) with “Prob > F" values imply that they are also statistically significant, with values less than 0.0500. However, if there are numerous non-significant terms (other than those required for the model hierarchy), it may be helpful to simplify the model to enhance its overall performance. The 0.34 standard deviation and 1.42 coefficient of variation (CV) imply low levels of variability and a limited range of values around the mean of 23.96. The greater R^2_{sqr} value of 0.9980 indicates that the model fits the data well and explains a considerable part of the variability in the dependent variable. Furthermore, the adjusted and forecast R^2_{sqr} values of 0.9971 and 0.9962, respectively, show that the model has a high capacity to predict future outcomes. The model’s predictive power is further supported by the model’s low PRESS (Prediction Sum of Squares) value of 2.26. The Statistical parameters described above is shown in Table 5b. The regression equation is also shown below.

Table 5a
ANOVA outcome for different parameters.

	BTE		EGT		CO		NOx		UBHC	
	F	p-value	F	p-value	F	p-value	F	p-value	F	p-value
Source	Value	Prob > F	Value	Prob > F	Value	Prob > F	Value	Prob > F	Value	Prob > F
Model	1022.45	<0.0001	1892.39	<0.0001	95.14	<0.0001	292.06	<0.0001	198.34	<0.0001
E	3522.16	<0.0001	9049.12	<0.0001	242.3	<0.0001	1376.14	<0.0001	800.43	<0.0001
L	70.44	<0.0001	40.233	<0.0001	117.61	<0.0001	1.2	0.3	59.1	<0.0001
EL	0.332	0.58	2.014	0.187	44.9	<0.0001	1.44	0.26	1.001	0.34
E^2	794.48	<0.0001	122.66	<0.0001	1.74	0.22	2.32	0.16	41.18	<0.0001
L^2	0.595	0.45	0.761	0.4	4.08	0.07	1.71	0.219	0.689	0.43

Table 5b
Statistical parameters for BTE.

Sl.No	Statistical parameter	Value
1	Std. Dev.	0.34
2	Mean	23.96
3	C.V. %	1.42
4	PRESS	2.26
5	R-Squared	0.9980
6	Adj R-Squared	0.9971
7	Pred R-Squared	0.9962
8	Adeq Precision	77.054

$$BTE = 5.688 + 0.62*L - 0.051*E - 0.000196*L*E - 0.00376*L^2 - 0.00159*E^2 \text{——} \tag{1}$$

Fig. 3 displays the impact of *EGR* rate on BTE of the POME-fueled CRDI DF engine adopted with *MIS*. Fig. 3 shows POME fuel operated at a constant *MIS* combination (40 + 20+40)gives lower BTE for all the loads as contrasted to diesel.This may be due to the delayed combustion process which leads to vaporization of fuel injected later with lower PP and HRR [27]. The incomplete combustion caused by the exhaust gases' substitution of O_2 with CO_2 results in a decrease in BTE of the engine with an increase in the EGR rate.

A higher value of BTE was attained when the engine was operated without arrangement. The BTE observed for SIS-adopted directly fueled engines is 32.25%. Similarly, the BTE observed for POME-fueled engines adopted with *MIS* in conjunction with varied *EGR* rates are 31, 30.45, 30.1, 29.5, and 29.1% for 0%, 5%, 10%, 15%, and 20% *EGR* respectively when operated at 80% load. An optimum *EGR* rate of 10% in conjunction with *MIS* adopted for POME has been recommended to set the optimum performance with minimum emission. When the *EGR* rate is increased beyond 10%, there may be increased emissions except for the oxides of nitrogen due to more dilution of the exhaust gases. But as in the case of *MIS* POME fuel operated a 2.99% penalty in the BTE obtained for a 10% *EGR* rate as compared to without *EGR* at 80% load.

3.2. *Effect of MIS and EGR rate on EGT*

The model has an F-value of 1892.40, indicating that it is significant (Table 5a). The likelihood of such a significant Model F-value occurring owing to random variations in the data is exceedingly low (0.01%). The "Prob > F" values can be used to determine the importance of model terms. If the value is less than 0.0500, the related model term is likely to be important. Model terms A, B, and A2 are all significant in this scenario. If the "Prob > F" value is greater than 0.1000, this indicates that the relevant model term is not important. The statistical results show that the data under consideration is highly precise and accurate. The low coefficient of variation (C.V.%) of 1.88 indicates that the data points are densely grouped around the mean value of 279.91, with minimal fluctuation. The high R-squared value of 0.9989 indicates that the model fits the data very well, explaining nearly all of the variability in the response variable. Furthermore, the adjusted R-squared value of 0.9984 indicates that the goodness of fit of the model is not unduly dependent on the number of predictors included in the model. Furthermore, the model's high predictive R-squared value of 0.9981 suggests that it is quite good at predicting future observations. The prediction residual error sum of squares (PRESS) of 504.29 indicates that the model's predictions are highly accurate, with very little departure from the observed data. Finally, the appropriate precision value of 105.651 indicates that the signal-to-noise ratio is strong and that the model's predictions are accurate and reliable. Overall, these statistical findings give significant support for the data's correctness and precision, as well as the model employed to evaluate it. The Statistical parameters described above is shown in Table 5c. The regression equation is also shown below in equation (2).

$$EGT = 119.8 + 1.2024*L - 0.993*E + 0.00746*L*E + 0.0228*L^2 - 0.0277E^2 \text{—} \tag{2}$$

The experiment is conducted at different loads to study the effect of *EGR* rate and injection schemes on the EGTs obtained from SIS-adopted diesel-fueled engines and *MIS*-adopted POME biodiesel-fueled CRDI engines as shown in Fig. 4. It is found that EGTs increase with an increase in load on the engine. DF engine gives lower EGT as compared to *MIS* adopted POME fueled biodiesel fueled engine due to its higher calorific value & improved combustion.

It is observed that EGT decreases with an increase in the rate of gas recirculation. This is due to the incomplete combustion process and increase in unburnt fuel. The constant retarded *IT* with increasing *EGR* was an effect on decreasing the average peak temperature

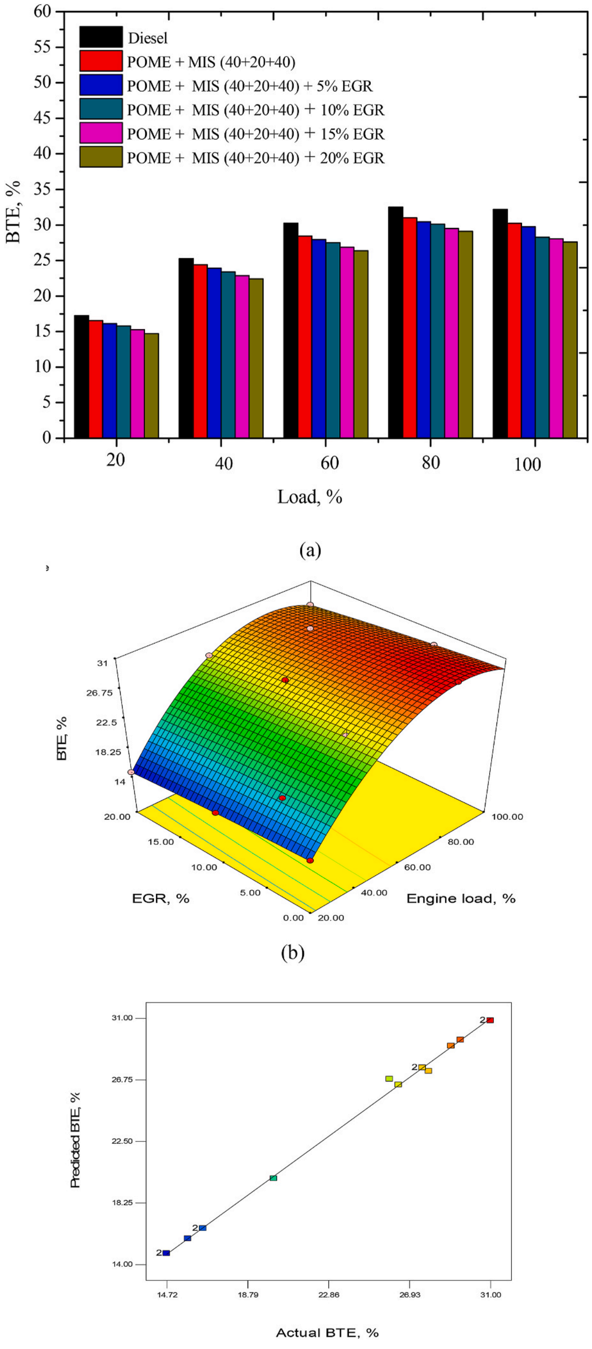

Fig. 3. Effect of MIS and EGR on BTE (a) Plot using Experiment values (b) 3-D surface plots using RSM (c) Model predicted vs Actual.

due to the linear surface being continuously subjected to the cooling oil effect of the piston moving upward. The observed results of EGT from the direct-fueled engine are 325 °C for diesel fuel when operated at 80% load. Similarly, the exhaust gas temperatures obtained for *MIS* adopted POME fueled engines with varied *EGR* rates are 357 °C, 352 °C, 346 °C, 341 °C, and 332 °C for 0%, 5%, 10%, 15%, and 20% *EGR* respectively under modified engine conditions when 80% load. However, a 3.08% reduction in EGT is obtained with a 10% *EGR* rate as compared to that obtained without *EGR* for 80% of the rated power.

Table 5c
Statistical parameters for EGT.

Sl.No	Perfomance parameter	Value
1	Std. Dev.	5.26
2	Mean	279.91
3	C.V. %	1.88
4	PRESS	504.29
5	R-Squared	0.9989
6	Adj R-Squared	0.9984
7	Pred R-Squared	0.9981
8	Adeq Precision	105.651

3.3. Effect of MIS and EGR rate on smoke opacity

The effect of MIS and EGR rate on the smoke opacity from SIS adopted DF engine and MIS-adopted POME biodiesel-fueled engine at different loads is shown in Fig. 5. Biodiesel fuel engine gives lesser smoke emiision at higher compression ratio and higher percentage of blend in diesel fuel [43,44]. Smoke level increases with an increase in the rate of gas recirculation due to the low oxygen concentration that leads to an incomplete combustion process for biodiesel fuel. The increase of smoke opacity with an increase in the EGR rate for the MIS adopted POME fueled engine is due to the deterioration of the AF ratio which leads to the poor combustion process. Smoke opacity obtained for DF and POME were 27 and 34 HSU respectively at 80% load. Thus, the smoke level increases by 25% from the POME-fuelled DF engine as compared to the DF engine. This is because of the relatively efficient combustion process in the diesel-fueled engine. The smoke level obtained for the MIS-adopted POME biodiesel fuel is 34, 38, 41, 43, and 48 HSU for 0%, 5%, 10%, 15%, and 20% EGR respectively under 80% load. Thus, 20.58% of the increase in smoke level is obtained with 10% of the EGR rate as compared to without EGR.

3.4. Effect of MIS and EGR rate on UBHC and CO emissions

The model for UBHC has an F-value of 198.34, indicating that it is extremely significant. A figure this enormous is extremely unlikely to occur by coincidence, having only a 0.01% probability of being noise. When the “Prob > F" values, which show the significance of each model term, are examined, it is discovered that terms A, B, and A2 are all significant with values less than 0.0500. This suggests that these terms have a substantial impact on the model and should be considered. The supplied statistical summary displays key metrics and measures of fit for a model or dataset. The standard deviation of 1.98 reflects the degree of data variability, with a smaller value representing greater consistency. The mean of 30.81 shows the data’s central tendency, or average value. The coefficient of variation (C.V.%) is a relative measure of variability that takes the magnitude of the mean into consideration. The R-squared value of 0.99 shows a high degree of correlation between the independent and dependent variables, with the model explaining 99% of the data variation. The adjusted R-squared value of 0.985 adjusts for the model’s predictor count and is frequently used to assess model complexity. The anticipated R-squared score of 0.9783 indicates the model’s prediction power on new data and can be used to evaluate its generalizability. The PRESS (predicted residual sum of squares) value of 85.34 represents the model’s error, with a lower number suggesting a better fit. The adequacy precision value of 37.944 is a statistic used to judge whether or not the model is accurate enough to meet the requirements of the analysis. Altogether, these indicators give a thorough evaluation of the model’s fit and predictive capacity, which may be used to guide additional analysis and decision-making. The Statistical parameters described above is shown in Table 5d. The regression equation is also shown below in equation (3).

$$UBHC = 13.25 - 0.167*L + 0.58*E + 0.00198*L*E + 0.00498*L^2 - 0.0099*E^2 — \tag{3}$$

The model for CO emissions has an F-value of 95.15, indicating that it is extremely significant (Table 5a). This suggests that there is a very minimal probability, about 0.01%, that such a high F-value may occur by chance or noise. Furthermore, when the “Prob > F" values are less than 0.0500, the model terms are statistically significant, indicating that they are not attributable to chance or noise. As a result, we may confidently conclude that the model is relevant and useful in forecasting the experiment’s outcome. The statistics reported in this data set indicate that the model has a high level of accuracy and precision.

The standard deviation, which quantifies the spread of data around the mean, is relatively tiny at 8.405E-003, implying that the data points are tightly grouped around the average value. The R-squared score is high at 0.9794, indicating that the model explains 97.94% of the variability in the response variable. At 0.9691, the adjusted R-squared value indicates that the model has good predictive potential and is not overfitting the data. The prediction R-squared value of 0.9512 indicates that the model is capable of producing accurate predictions in the future. The PRESS score of 1.675E-003 indicates that the model has a low sum of squared prediction errors, which supports the model’s correctness. The appropriate precision score of 28.005 indicates that the signal-to-noise ratio for the model is adequate, indicating a high level of confidence in the results. These statistics indicate that the model is resilient and dependable, and that it can be utilised to make accurate predictions. The Statistical parameters described above is shown in Table 5e. The regression equation is also shown below in equation (4).

$$CO = 0.0129 + 0.00109*L + 0.0043*E - 0.000056*L*E + 0.000004*L^2 + 0.000103*E^2 — \tag{4}$$

The effect of the EGR rate on UBHC & CO emissions from SIS-adopted diesel-fueled engines and MIS-adopted POME-fuelled diesel engines is shown in Figs. 6 and 7. Generally, CO emission increases as the number of holes increases in the nozzle. CO emission

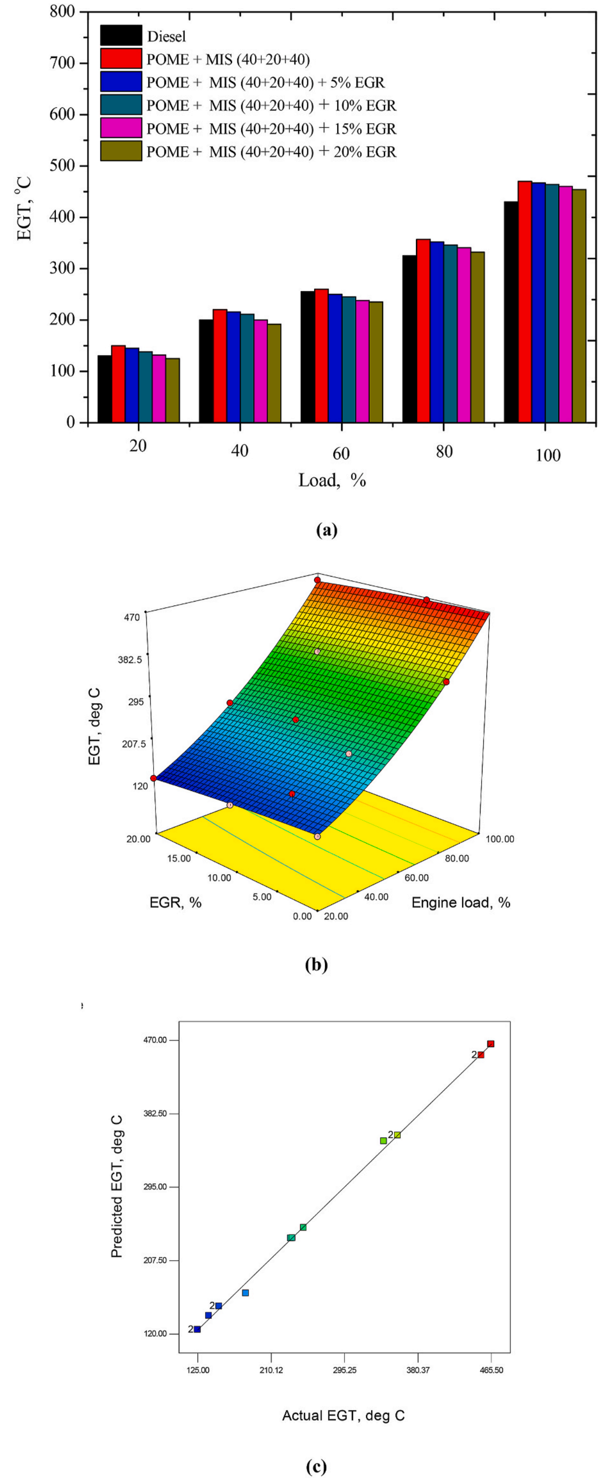

Fig. 4. Effect of MIS and EGR on exhaust gas temperature (a) Plot using Experiment values (b) 3-D surface plots using RSM (c) Model predicted vs Actual.

increases due to prolonged ignition delay at the higher EGR rate as the smaller number of nozzle holes leads to improving the over-mixing AF ratio. The emissions will be reduced close to the pilot fuel injection of MIS because of the local AF ratio turning into an over-lean mixture region at a lower temperature But CO emission increases during the post-fuel injection due to the high-temperature rate. UBHC emissions also reduce at close pilot fuel injection but increase during the post-fuel injection due to the more amount of the fuel being injected at high temperature. The fuel does not get sufficient time to mix with air and is burned in a high equivalence ratio. Thus

Table 5d
Statistical parameters for UBHC.

Sl.No	Perfomance parameter	Value
9	Std. Dev.	1.98
10	Mean	30.81
11	C.V. %	6.44
12	PRESS	85.34
13	R-Squared	0.9900
14	Adj R-Squared	0.9850
15	Pred R-Squared	0.9783
16	Adeq Precision	37.944

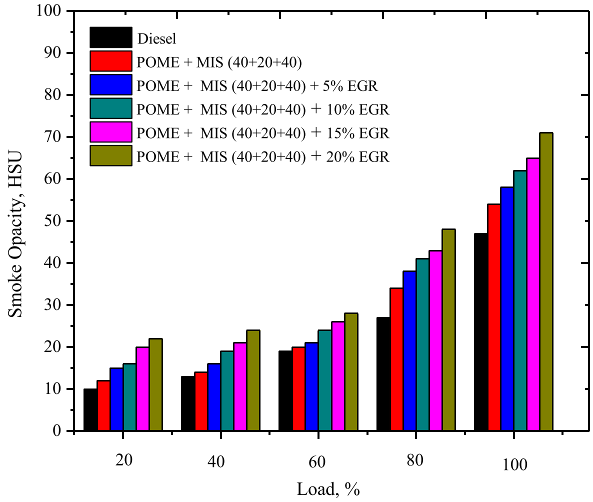

Fig. 5. Effect of MIS and EGR on smoke emission.

both CO and UBHC emissions obtained from the MIS adopted POME fueled engine is more because of the delayed combustion process and the vaporization of the fuel injected later during the post-fuel injection. 28 ppm and 32 ppm of UBHC emissions were observed in the exhaust gas from the direct fueled engine and the POME fueled engine with 0% EGR respectively. Whereas, the CO emissions were 0.11 and 0.12 vol percentages respectively. UBHC emission increases by 13.33% with a 10% of EGR rate as compared to 0% of EGR for POME-fueled diesel engines. Similarly, CO emission increases by 15.45% with 10% of the EGR rate as compared to 0% of EGR for the POME-fueled diesel engine.

3.5. *Effect of MIS and EGR rate on oxides of nitrogen*

The Model F-value of 292.07 indicates that the model is significant and is unlikely to emerge as a result of random fluctuations (Table 5a). In fact, the likelihood of such a huge Model F-value occurring by chance is merely 0.01%.

When examining the model term's significance, values of “Prob > F" less than 0.0500 suggest that the terms are statistically significant. In this situation, term A is a substantial model term, which means it has a large impact on the outcome under consideration. The numbers provided represent the performance of a model that appears to have a high level of accuracy based on its R-squared value of 0.9932. This number implies that the independent variables in the model can explain about 99.32% of the variance in the dependent variable. The mean value of 531.16 implies that the dependent variable's average value is around 531.16. The coefficient of variation (CV) of 6.54% indicates that the dependent variable's standard deviation is low in comparison to its mean. Furthermore, the model's adjusted R-squared and predicted R-squared values of 0.9898 and 0.9867, respectively, indicate that the model is well-fitting and

Table 5e
Statistical parameters for CO.

Sl.No	Perfomance parameter	Value
1	Std. Dev.	8.405E-003
2	eMean	0.12
3	C.V. %	6.94
4	PRESS	1.675E-003
5	R-Squared	0.9794
6	Adj R-Squared	0.9691
7	Pred R-Squared	0.9512
8	Adeq Precision	28.005

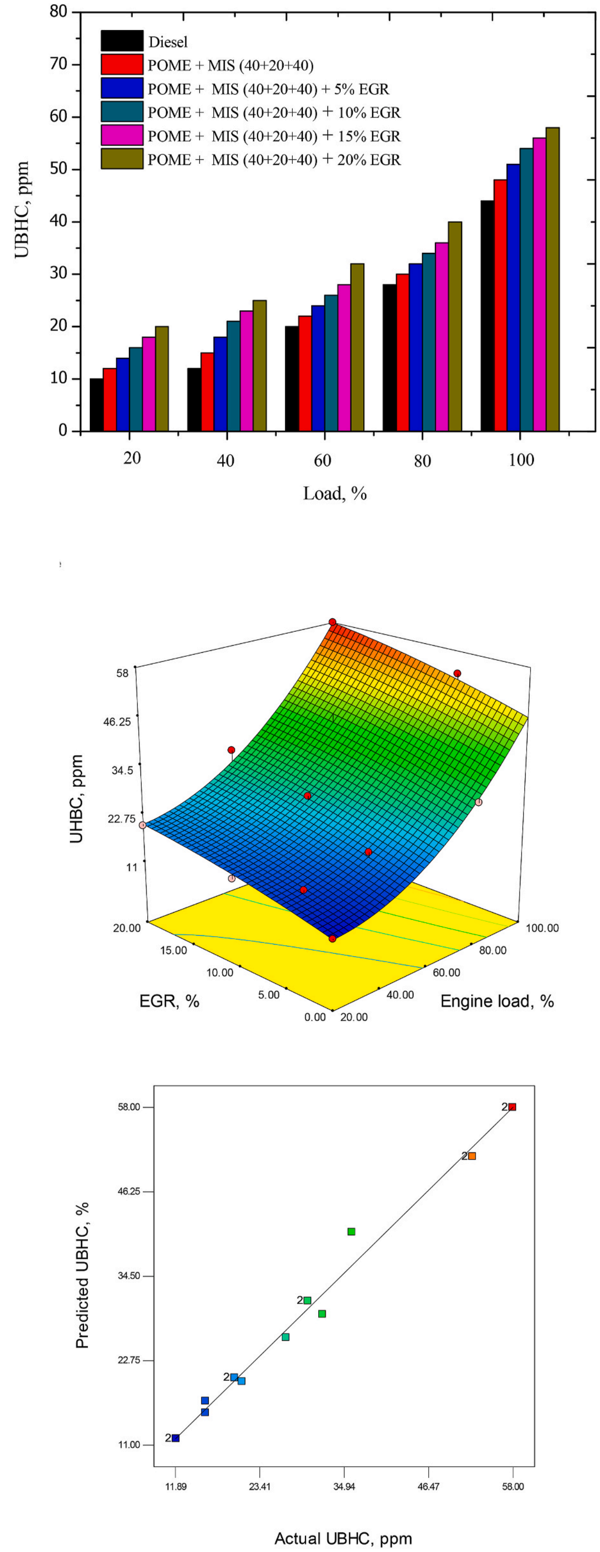

Fig. 6. Effect of MIS and EGR on UBHC emission (a) Plot using Experiment values (b) 3-D surface plots using RSM (c) Model predicted vs Actual.

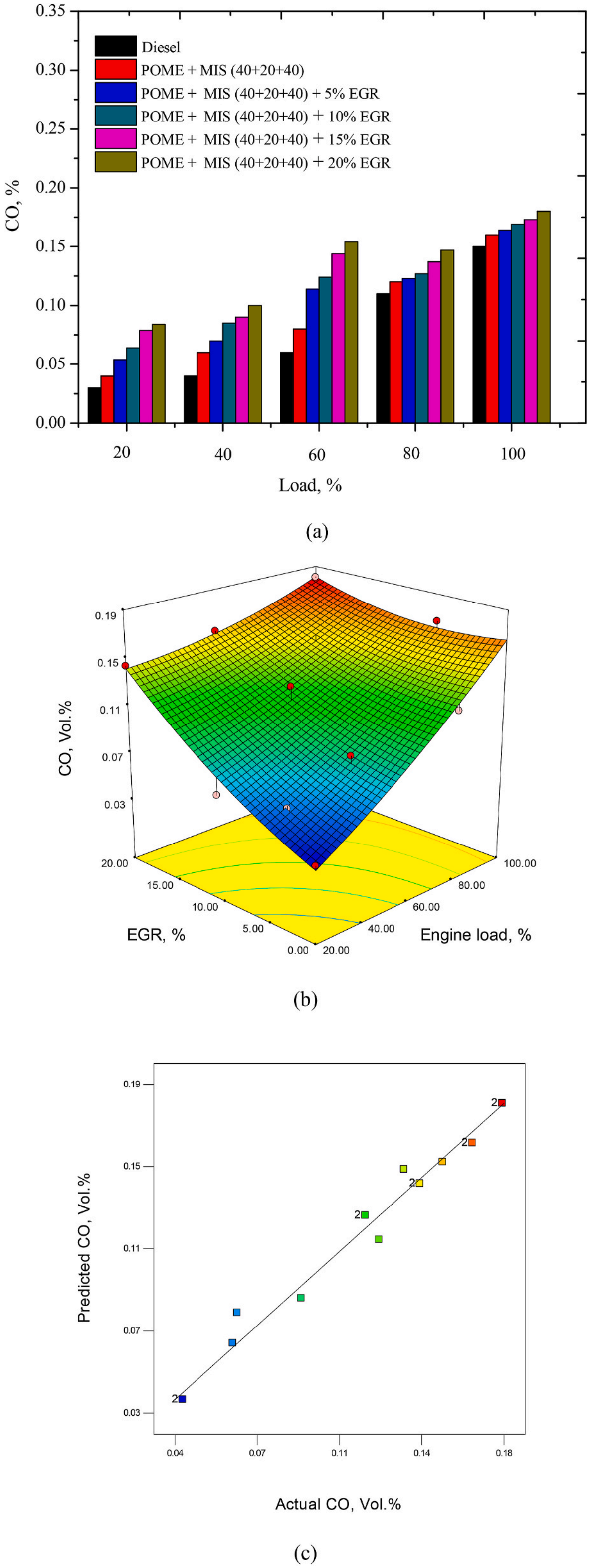

Fig. 7. Effect of MIS and EGR on CO emission (a) Plot using Experiment values (b) 3-D surface plots using RSM (c) Model predicted vs Actual.

Table 5f
Statistical parameters for NOx.

Sl.No	Perfomance parameter	Value
1	Std. Dev.	5.26
2	Mean	531.16
3	C.V. %	6.54
4	PRESS	23588.90
5	R-Squared	0.9932
6	Adj R-Squared	0.9898
7	Pred R-Squared	0.9867
8	Adeq Precision	39.476

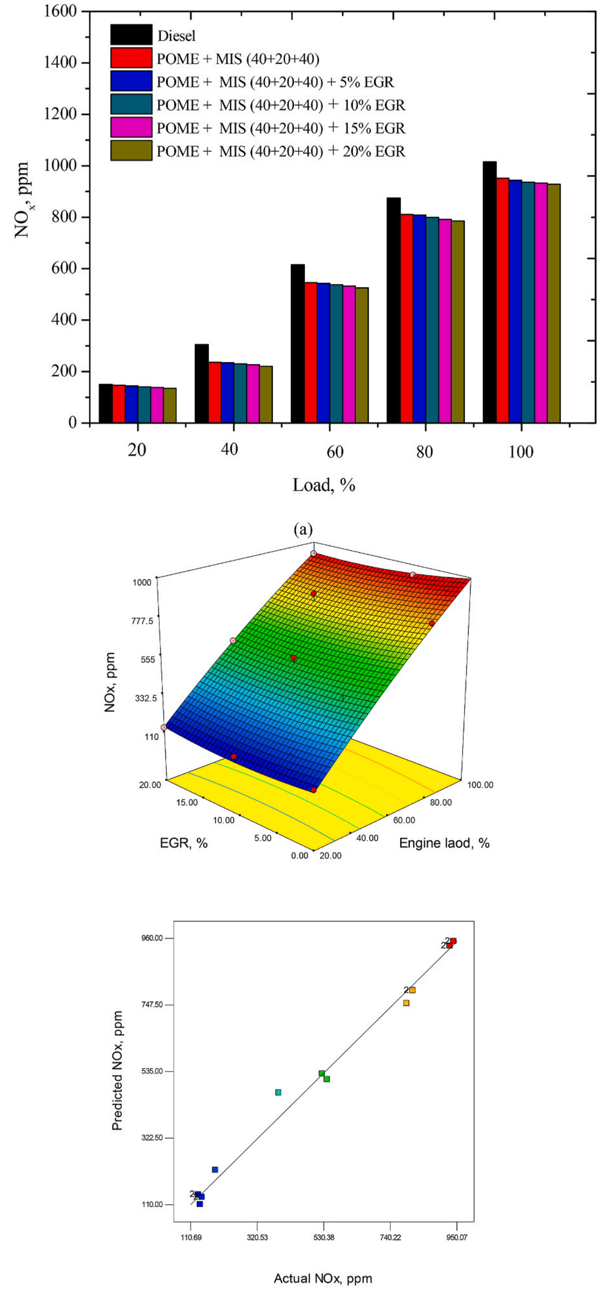

Fig. 8. Effect of MIS and EGR on NO_x emission (a) Plot using Experiment values (b) 3-D surface plots using RSM (c) Model predicted vs Actual.

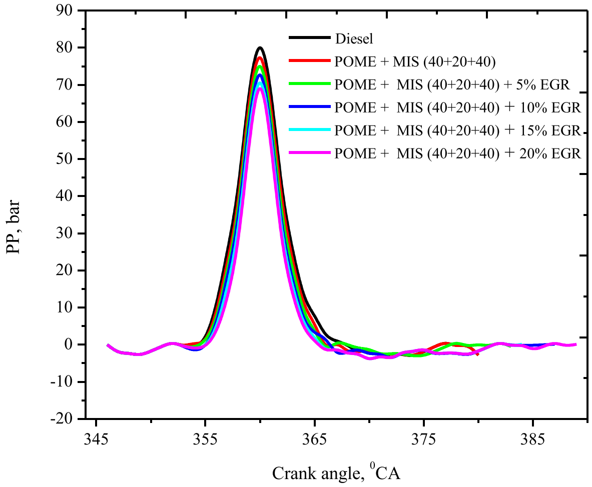

Fig. 9a. Effect of MIS and EGR on peak pressure.

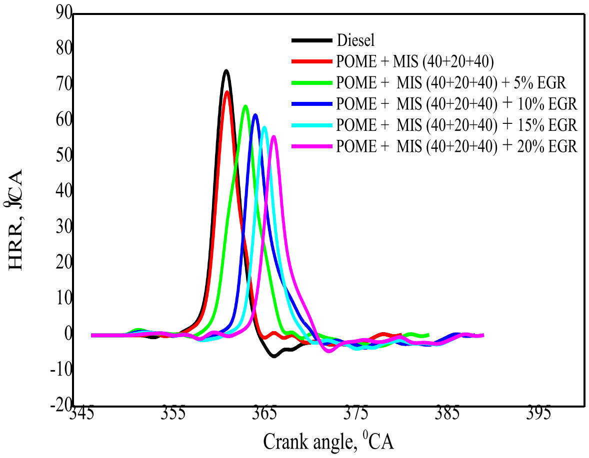

Fig. 9b. Effect of MIS and EGR on heat release rate.

predictive. The model's PRESS value of 23588.90, on the other hand, indicates that there is some level of error between the predicted and actual values of the dependent variable. Finally, the model's adequate precision of 39.476 indicates that the model's signal-to-noise ratio is reasonably high, implying that the model can make precise predictions. Overall, the results indicate that the model has a good level of accuracy and predictive capacity, with some prediction error. The Statistical parameters described above is shown in Table 5f. The regression equation is also shown below in equation (5).

$$NOx = -122.48 + 13.24*L - 4.26*E - 0.0417*L*E - 0.021*L^2 + 0.275*E^2 \qquad (5)$$

The effect of *EGR* on NO_x formation from both the SIS and *MIS*-adopted diesel engines at different loads is shown in Fig. 8. The exhaust gas recirculated mixes with fuel-air mixture in the cylinder. The thermal capacity of the mixture increases which reduces the temperature of the burning mixture which results in the decrease of NO_x formation. CO_2 present in the exhaust gases will replace the O_2 present in the fuel-air mixture and hence decreases the soot formation. The burning of the pilot-injected fuel reduces the ID period which minimizes the intensity of the premixture combustion suppressing the temperature and decreasing the NO_x formation [28]. The late *IT* and more quantity of fuel injected increase the NO_x emission. The higher *EGR* rate in conjunction with *MIS* will extend the ID which tends to more premixed in-cylinder conditions and lower temperatures obtained. This enables to reduce the NO_x emission. Thus, *MIS* in conjunction with *EGR* reduces the overall NO_x emission at higher *IOP* [29]. Nitrogen oxide emissions of 875 ppm and 811 ppm were obtained from the diesel-fueled engine and POME biodiesel-fueled engine respectively. Thus, NO_x is reduced by 7.31% from *MIS* adopted POME diesel engine as compared to SIS adopted diesel engine. The NO_x is reduced by 1.35% from the POME-fuelled diesel engine with 10% *EGR* as compared to that with 0% *EGR* when the engine operated at 80% load.

Table 5g
L16 Orthogonal array.

Trial No.	BP (kW)	EGR (%)
1	2.08	5
2	2.08	10
3	2.08	15
4	2.08	20
5	3.12	5
6	3.12	10
7	3.12	15
8	3.12	20
9	4.16	5
10	4.16	10
11	4.16	15
12	4.16	20
13	5.20	5
14	5.20	10
15	5.20	15
16	5.20	20

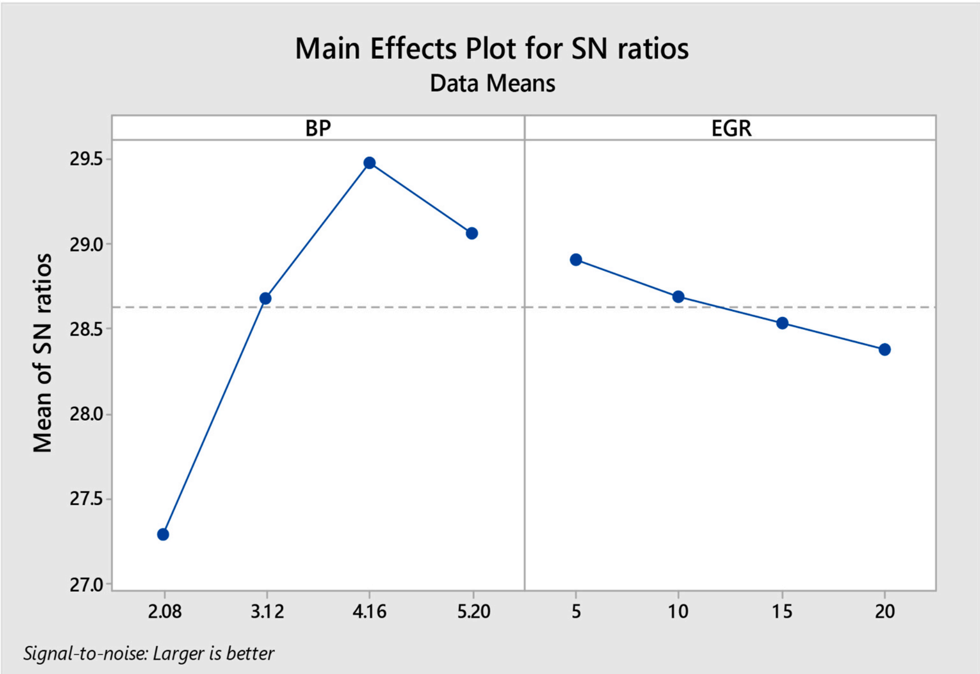

Fig. 10a. Effect of SN ratios with BP and EGR for BTE.

3.6. *Effect of MIS and EGR rate on combustion characteristics*

The effect of the EGR rate on the inline cylinder PP and HRR of both SIS and MIS-adopted fueled engines is shown in Fig. 9a and b. While the combustion of the fuel injected in the first pulse is still going on, the main injection occurs, PP and HRR increase slowly during the initial period and attain a maximum value while approaching the top dead centre due to longer ID which gives more time for mixing the air and fuel. The use of EGR in conjunction with MIS will lead to a longer ignition delay with more time for mixing. Thus, high EGR and post-injection of the MIS will help to control the NO_x, soot and other emissions. The higher IOP was used to increase the quality of the combustion process by ensuring good mixture formation during an ID period and the oxygen content of POME is 10.8. The higher IOP of 7 NIG improves fuel atomization and fuel injection rate. This, in turn, advances combustion phasing, decreases the ID and increases the peak HRR. Hence, higher NO_x emitted at higher IOP, this NO_x would be controlled by EGR and MIS. However, DF and POME showed PP up to 85 bar and 83 bar respectively. The 2.40% reduction in PP as compared to DF at 0% of EGR and 4.81% of PP reduced for 10% of EGR as compared to 0% of EGR for MIS operation of POME BDF. Similarly, 8.75% of HRR was reduced by 10% of EGR as compared to 0% of EGR for the MIS.

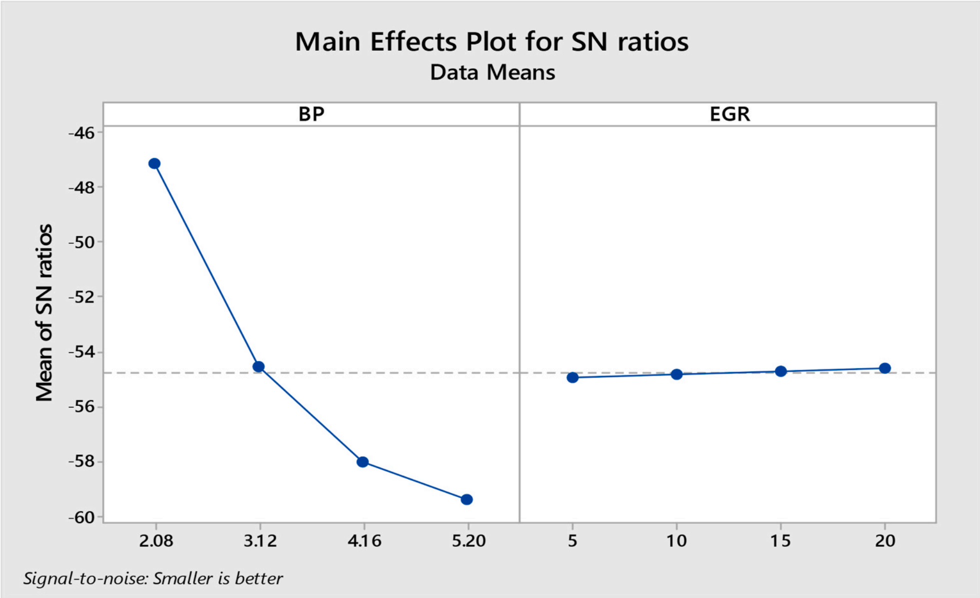

Fig. 10b. Effect of SN ratios with BP and EGR for NO_x.

Table 6
Optimum operational conditions using Desirability approach.

Load	EGR	BTE	EGT	CO	NOx	UBHC	Desirability	
80	4.67	30.51798	359.4828	0.129519	774.7055	34.97755	0.654232	Selected

3.7. *Design of experiments by Taguchi method and its analysis*

The design of the experiment is employed to conduct the design of the experiments to be carried out on the modified engine set-up. The main objective is to optimize the *EGR* rate in a modified setup, the two influencing factors such as *EGR* and BP are selected. BTE and NO_x are response variables for the influencing factors. The L16 orthogonal array was selected to design the experiments shown in Table 5g. The *EGR* rate of the engine is optimized under the following engine conditions Number of holes of injector: 7, speed: 1500 rpm, CR: 17.5, *IT*: 10^{o}bTDC, *IOP*: 900 bar, *MIS*:40 + 20+40, and CCS: TRCC.The combination of 80% of the load (4.16 kW) and 5% *EGR*

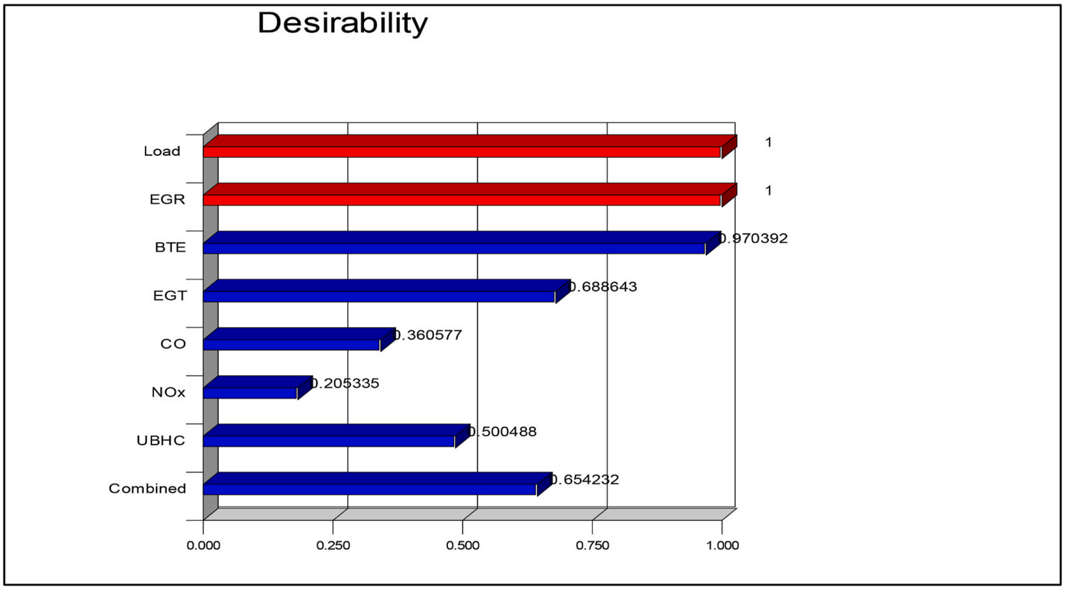

Fig. 10c. Desirability values.

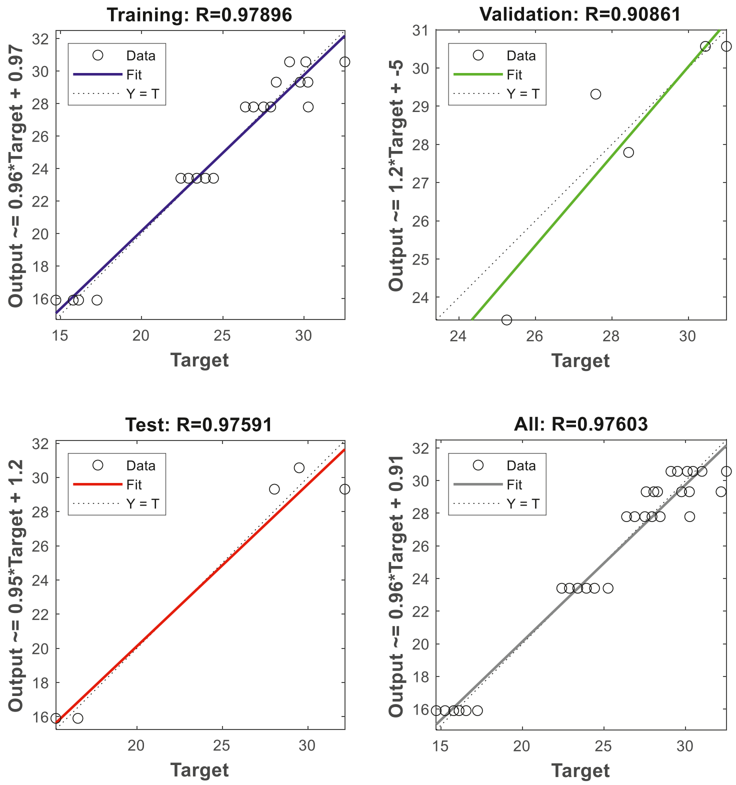

(i) BTE

Fig. 10d. Regression fit for the training, validation, and test sets.

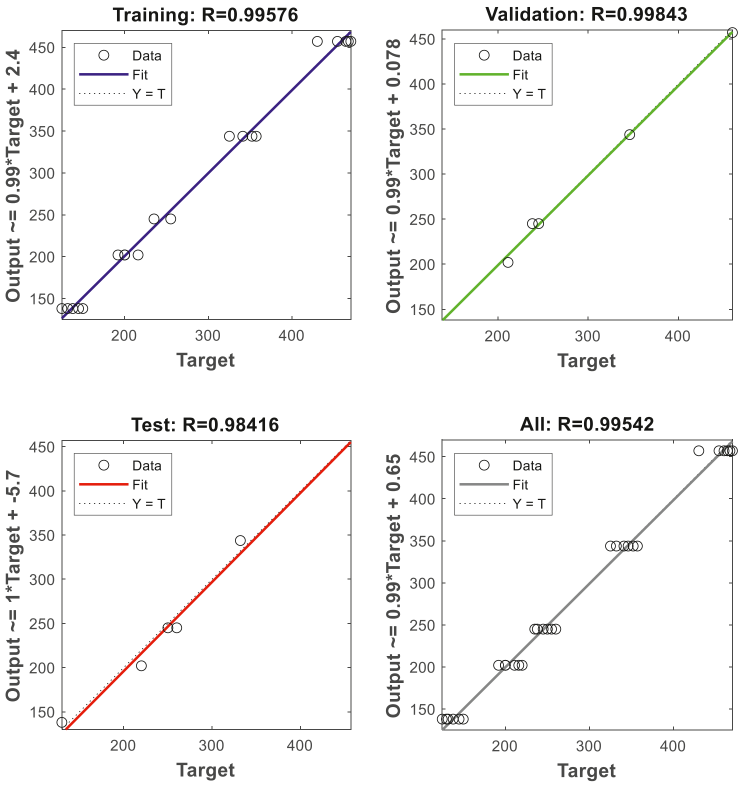

(ii) EGT

Fig. 10d. (*continued*).

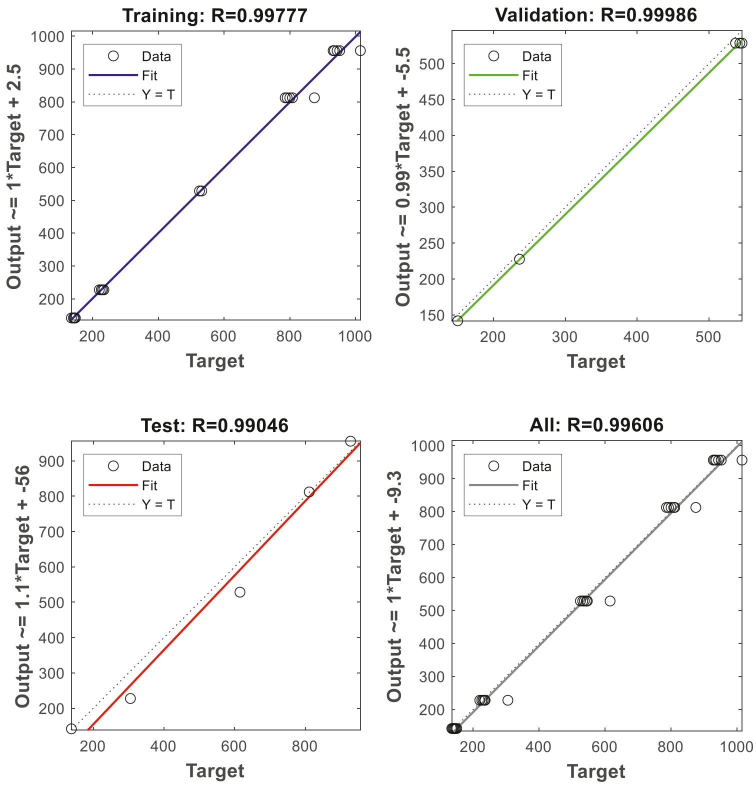

(iii) NOx

Fig. 10d. (*continued*).

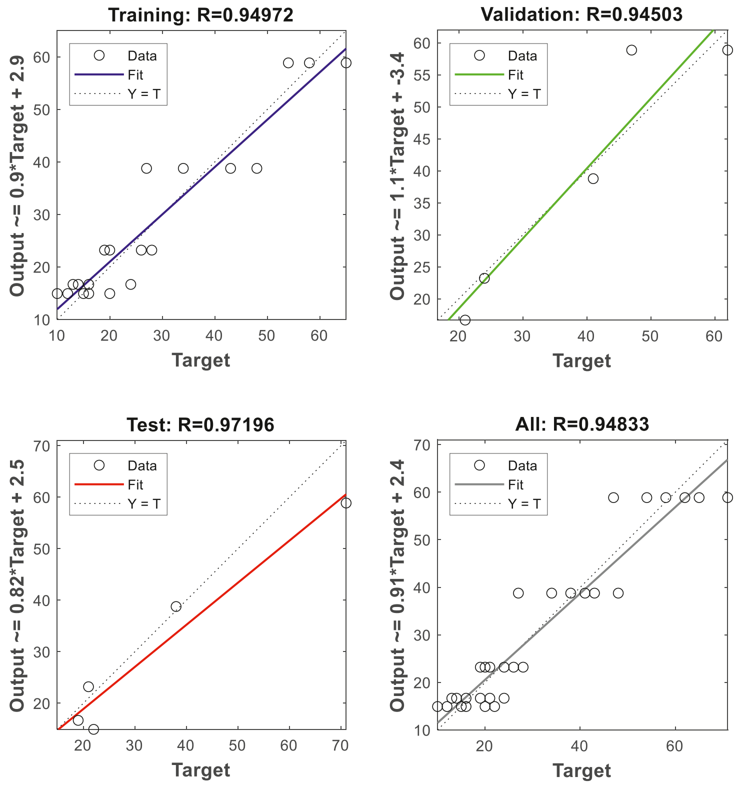

(iv) Smoke

Fig. 10d. (*continued*).

rate has been optimized by the Taguchi method due to higher the SN ratio as indicated in Fig. 10a. As comparing both factors, analysis shows that the higher influencing factor is BP. Usually, 10–15% of the *EGR* rate can be supplied with a penalty of BTE in the engine. Fig. 10b shows the NO_x is showing better at 100% load with a 5% *EGR* rate due to smaller is better. However, BP is more influential than *EGR* in the analysis.

3.8. Optimization using desirability approach

To get the best possible combination of output parameters, such as BTE, NOx, carbon monoxide, and HC, in the current study, independent control parameters, such as engine load, oxyhydrogen flow rates, and pilot injection timing, were optimized using a desirability method. All inputs were transformed into a dimensionless desirability value (z), which ranged from 0 to 1. An unacceptable outcome is denoted by a desirability value of $z = 0$, whereas an excellent outcome is denoted by $z = 1$. Each result's objective is either to minimize, maximize, or remain equal, depending on the issue's criteria. In this study, the maximum BTE was desired, the exhaust emission indices were kept to a minimum, and all three control factors were maintained within the range.

The desirability values assigned to each study variable are described in Table 6. The optimisation technique involves combining multiple outputs into the function of desirability(FD), a dimensionless performance entity. Fig. 10c displays the desirability values obtained in this study. An effective way to determine the ideal set of input parameters that can produce the desired output is to apply the multi-input/output optimisation technique using the desirability approach. The findings of this study can be used to improve the performance of diesel engines in transportation systems, and further research could look at the technique's economic advantages.

3.9. Model predictability assessment

From the input and output variables, ANN was used to build the multiple regression model. In Fig. 10d, the whole regression fit for the training, validation, and test sets is shown. The near proximity of the values for the training, validation, test, and overall correlation coefficients to 1 illustrates the great accuracy of the ANN model's output responses [31].

4. Conclusions

The results could be drawn from the experiments conducted with varied EGR rates powered by POME fuel at IT 10° bTDC, IOP 900 bar, 7holesNIG and MIS combination of 40-20-40 with TRCC shape.

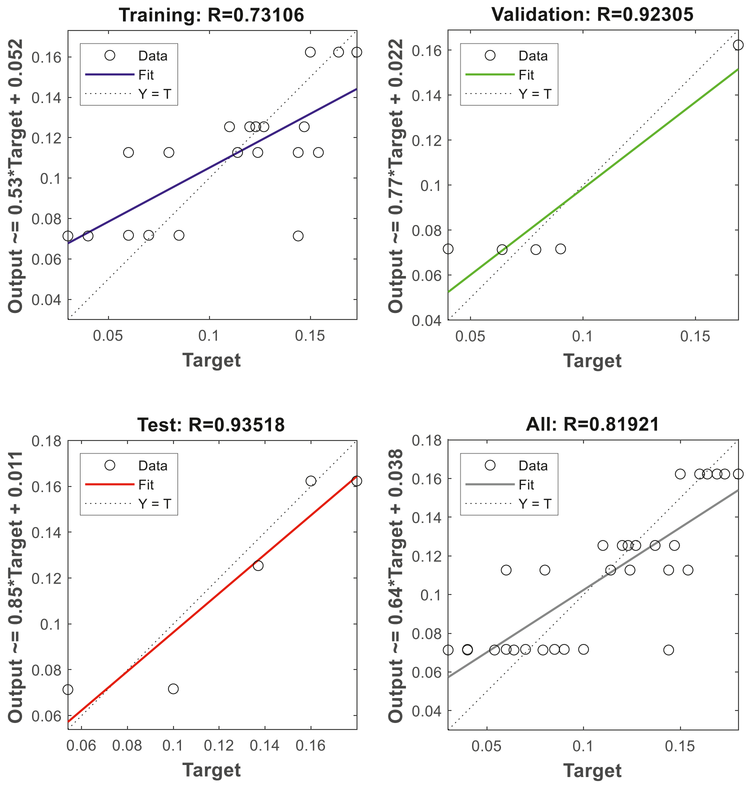

(V) Co

Fig. 10d. (*continued*).

- From DOE it is observed that the optimized values of load and EGR rate are 80% and 5% respectively for improvement in performance and reduction in NO x emissions. However, 10% of EGR has been selected to gain nominal NO x emission with a penalty of BTE in the modified POME-operated CRDI engine.
- A 1.35% of reduction in NO x is achieved with a penalty of 2.90% in the value of Brake Thermal Efficiency for an EGR rate of 10% as compared to without the EGR rate. MIS adopted a POME-fuelled diesel engine with 10 EGR giving a reduction of PP and HRR by 4.81 and 8.75% respectively as compared to without EGR.
- MIS adopted a POME-fuelled diesel engine with 10% EGR giving an increase in UBHC, CO and smoke emissions. CO, UBHC and smoke emissions increased by 5.8%, 13.33%, and 20.58% respectively as compared to without EGR.
- For an EGR rate of 20%, it is observed that 3.1% reductions in NOx are achieved with a penalty of 6.1% in the value of brake thermal efficiency and with the increase in emissions such as CO, UBHC and smoke emissions by 22.5, 33.3 and 41% respectively as compared to without EGR. An optimal EGR rate of 10% is chosen such that the tradeoff is done concerning smoke and NOx emissions with acceptable engine performance.
- The Operating parameters such as MIS selection, IT, fuel injection amount and duration, IOP, nozzle geometry, and EGR rate can be judiciously selected for a given fuel and combustion chamber shape for the improvement in performance and acceptable level of emissions.
- MIS along with EGR is an effective method for the reduction of NOx emissions but with a penalty in the value of BTE and an increased amount of unburnt fuel.
- Both the ANN and RSM models correctly fit the experimental data, producing R^2 values that ranged from 95.5% to 98.5%, respectively.
- The findings show that RSM and ANN are both highly accurate modelling approaches. Additionally, as compared to RSM, the ANN model's predictive accuracy was marginally better.

These findings have a great deal of application potential in diesel-powered transportation systems. Examining the economic aspects connected to the ideal operating parameters must, however, be a future focus of the research.

5. Scope for future work

Biodiesel fuel can be used as an alternative fuel in a DF engine to save a huge amount of fossil fuel requirements worldwide. The research work can be carried in feature with suitable modification in the CRDI biodiesel fuelled diesel engine.

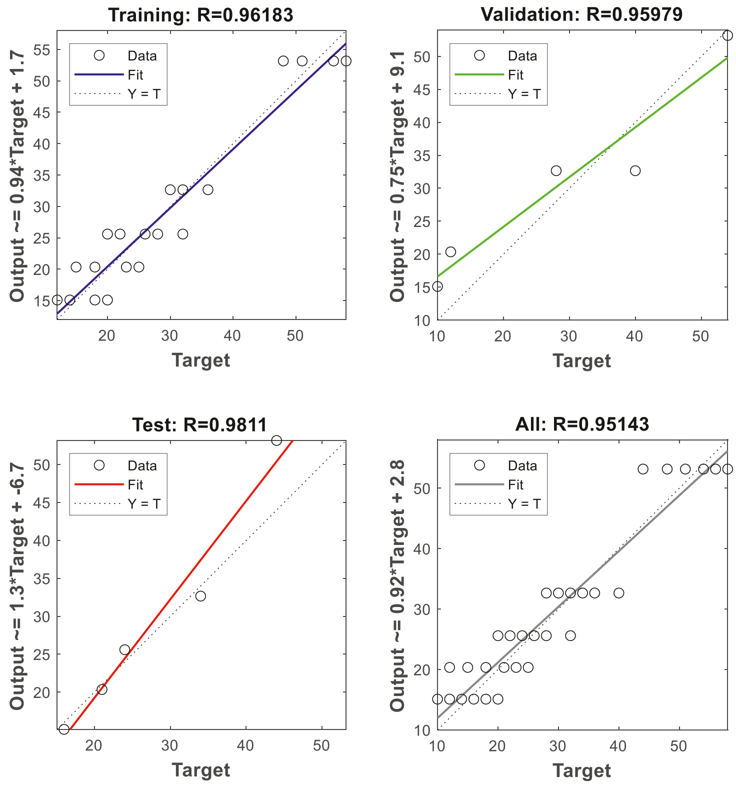

(vii) UBHC

Fig. 10d. (*continued*).

1. Different biodiesel fuels can be used to optimize the combination of injection strategies and combustion chamber shape in modern biodiesel fuel operated diesel engine with CFD techniques.
2. Turbocharged arrangement can be used to boost up the power of the biodiesel fueled diesel engine.
3. The theoretical mathematical modelling technique can be used to optimize both the combination of injection strategies and CCS on biodiesel engine performance.

Author statement

Alur S A: Conceptualization, Methodology. **Shivashimpi M M:** Data curation, Writing- Original draft preparation. **J. Samson Isaac:** Visualization, Investigation. **Banapurmath N R***:* Supervision. **D. Sakthivel:** Software, Validation. **Yogesh Diliprao Sonawane:** Writing- Reviewing and Editing **Prabhakar Sharma:** Formal analysis. **Mohammad Amir Khan:** Resources. **Saiful Islam:** Data Curation. **Abdul Razak:** Supervision.

Declaration of competing interest

The authors declare that there is no conflict of interest.

Data availability

Data will be made available on request.

Acknowledgement

The authors extend their appreciation to the Deanship of Scientific Research at King Khalid University for funding this work through large group Research Project under grant number RGP2/556/44.

References

[1] Upendra Rajak, Thokchom Subhaschandra Singh, Tikendra Nath Verma, Prem Kumar Chaurasiya, Saboor Shaik, Asif Afzal, Erdem Cuce, Ali A. Rajhi, C. Ahamed Saleel, Experimental and parametric studies on the effect of waste cooking oil methyl ester with diesel fuel in compression ignition engine, Part C, Sustain. Energy Technol. Assessments 53 (2022), 102705, https://doi.org/10.1016/j.seta.2022.102705. ISSN 2213-1388.
[2] G.S. Hebbar, NO_x from diesel engine emission and control strategies-a review, Int. J. Mech. Eng. Robotics Res. 3 (4) (2014) 471.
[3] P. Appavu, M.V. Ramanan, J. Jayaraman, H. Venu, NO_x emission reduction techniques in biodiesel-fuelled CI engine: a review, Aust. J. Mech. Eng. 8 (2019), 1-1.
[4] P. Tamilselvan, G.G. Srinivasu, Performance, emission and combustion characteristics of VCR CRDI diesel engine fuelled with n-butanol blends, Int. J. Automot. Mech. Eng. 16 (3) (2019 3) 6825–6843.
[5] D. Wang, C. Zhang, Y. Wang, A numerical study of multiple fuel injection strategies for NOx reduction from DI diesel engines, Int. J. Green Energy 4 (4) (2007) 453–470.
[6] M.A. Mossa, A.A. Hairuddin, A.A. Nuraini, J. Zulkiple, H.M. Tobib, Effects of hot exhaust gas recirculation (EGR) on the emission and performance of a single-cylinder diesel engine, Int. J. Automot. Mech. Eng. 16 (2) (2019) 6660–6674.
[7] S. Saravanan, G. Nagarajan, S. Sampath, Combined effect of injection timing, EGR and injection pressure in reducing the NO_x emission of a biodiesel blend, Int. J. Sustain. Energy 33 (2) (2014) 386–399.
[8] U. Rajak, A. Dasore, P.K. Chaurasiya, et al., Effects of microalgae -ethanol-methanol-diesel blends on the spray characteristics and emissions of a diesel engine, Environ. Dev. Sustain. 25 (2023) 1–22, https://doi.org/10.1007/s10668-021-01998-6.
[9] M.V. De Poures, A.P. Sathiyagnanam, D. Rana, B.R. Kumar, S. Saravanan, 1-Hexanol as a sustainable biofuel in DI diesel engines and its effect on combustion and emissions under the influence of injection timing and exhaust gas recirculation (EGR), Appl. Therm. Eng. 113 (2017) 1505–1513.
[10] S. Pai, A. Sharief, S. Kumar, Influence of ultra-injection pressure with dynamic injection timing on CRDI engine performance using Simarouba biodiesel blends, Int. J. Automot. Mech. Eng. 15 (4) (2018) 5748–5759.
[11] C.S. Aalam, C.G. Saravanan, B.P. Anand, Impact of high fuel injection pressure on the characteristics of CRDI diesel engine powered by mahua methyl ester blend, Appl. Therm. Eng. 106 (2016) 702–711.
[12] S.V. Khandal, N.R. Banapurmath, V.N. Gaitonde, V.S. Yaliwal, Common rail direct injection mode of CI engine operation with different injection strategies-A method to reduce smoke and NOx emissions simultaneously, European J. Sustain. Develop. Res. 2 (2) (2018) 15.
[13] R.S. Shukla, A.D. Shetty, A.J. Antony, Performance and emission characteristics of CRDI engine working on plastic oil, Indian J. Sci. Technol. 9 (45) (2016) 1–6.
[14] A.K. Agarwal, A. Dhar, J.G. Gupta, W.I. Kim, K. Choi, C.S. Lee, S. Park, Effect of fuel injection pressure and injection timing of Karanja biodiesel blends on fuel spray, engine performance, emissions and combustion characteristics, Energy Convers. Manag. 91 (2015) 302–314.
[15] A.K. Agarwal, A. Dhar, J.G. Gupta, W.I. Kim, S. Le, Park, Effect of fuel injection pressure and injection timing on spray characteristics and particulate size–number distribution in a biodiesel fuelled common rail direct injection diesel engine, Appl. Energy 130 (2014) 212–221.
[16] M.M. Shivashimpi, N.R. Banapurmath, S.A. Alur, B.M. Dodamani, Optimisation of nozzle geometry in the modified common rail direct injection biodiesel-fuelled diesel engine, Int. J. Ambient Energy 1 (2019) 1–9.
[17] D.H. Qi, K. Yang, D. Zhang, B. Chen, Combustion and emission characteristics of diesel-tung oil-ethanol blended fuels used in a CRDI diesel engine with different injection strategies, Appl. Therm. Eng. 111 (2017) 927–935.
[18] A. Dhar, A.K. Agarwal, Experimental investigations of the effect of pilot injection on performance, emissions and combustion characteristics of Karanja biodiesel fuelled CRDI engine, Energy Convers. Manag. 93 (2015) 357–366.
[19] R. Sindhu, G.A. Rao, K.M. Murthy, Effective reduction of NO_x emissions from diesel engine using split injections, Alex. Eng. J. 57 (3) (2018) 1379–1392.
[20] [18] P. Punov, T. Gechev, S. Mihalkov, P. Podevin, D. Barta, Experimental study of multiple pilot injection strategy in an automotive direct injection diesel engine, MATEC Web of Conferences 234 (2018), 03007.
[21] S.H. Park, S.H. Yoon, C.S. Lee, Effects of multiple-injection strategies on overall spray behavior, combustion, and emissions reduction characteristics of biodiesel fuel, Appl. Energy 88 (1) (2011) 88–98.
[22] W. Park, Y. Ra, E. Kurtz, W. Willems, R.D. Reitz, Use of multiple injection strategies to reduce emission and noise in low temperature diesel combustion, SAE Technical Paper (2015) 14.
[23] B. Prem Anand, S. Prasanna Raj Yadav, B. Aasthiya, G. Akshaya, K. Arulmozhi, Effect of fuel injection strategies on the performance of the common rail diesel injection (CRDI) engine powered by biofuel, Int. J. Ambient Energy 41 (14) (2020) 1577–1586.
[24] S.V. Khandal, Y. Tatagar, I.A. Badruddin, A study on performance of common rail direct injection engine with multiple-injection strategies, Arabian J. Sci. Eng. 45 (2) (2020) 623–630.
[25] B. Yin, J. Wang, K. Yang, H. Jia, Optimization of EGR and split injection strategy for light vehicle diesel low temperature combustion, Int. J. Automot. Technol. 15 (7) (2014) 1043–1051.
[26] M. Shivashimpi, S. Alur, N. Banapurmath, U. Kapale, Optimization of multiple injection strategy in modified common rail direct injection diesel engine powered with palm oil methyl ester, Int. J. Comput. Theor. Chem. 7 (1) (2019) 87.
[27] P. Sharma, D. Balasubramanian, C. Thanh Khai, I. Papla Venugopal, M. Alruqi, J.S.F. Josephin, A. Sonthalia, et al., Enhancing the performance of renewable biogas powered engine employing oxyhydrogen: Optimization with desirability and D-optimal design, Fuel 341 (2023) 127575.
[28] Donghui Qi, Michael Leick, Yu Liu, Chia-fon F. Lee, Effect of EGR and injection timing on combustion and emission characteristics of split injection strategy DI-diesel engine fueled with biodiesel, Fuel 90 (5) (2011) 1884–1891.
[29] S.V. Khandal, A. Razak, I. Veza, A. Afzal, M. Alwetaishi, S. Shaik, Ü. Ağbulut, A. Rashedi, Hydrogen and dual fuel mode performing in engine with different combustion chamber shapes: Modelling and analysis using RSM-ANN technique, Int. J. Hydrogen Energy (2022).
[30] V.K. Viswanathan, A.R. Kaladgi, P. Thomai, Ü. Ağbulut, M. Alwetaishi, Z. Said, S. Shaik, A. Afzal, Hybrid optimization and modelling of CI engine performance and emission characteristics of novel hybrid biodiesel blends, Renew. Energy 98 (2022) 549–567.
[31] A. Afzal, R.G. Roy, C.P. Koshy, Y. Alex, M. Abbas, E. Cuce, R.K. Abdul Razak, S. Shaik, C.A. Saleel, Characterization of biodiesel based on plastic pyrolysis oil (PPO) and coconut oil: Performance and emission analysis using RSM-ANN approach, Sustain. Energy Technol. Assessments 56 (2023) 103046.
[32] Muammer Özkan, Derya Burcu Özkan, Orkun Özener, Yılmaz Hasan, Experimental study on energy and exergy analyses of a diesel engine performed with multiple injection strategies: effect of pre-injection timing, Appl. Therm. Eng. 53 (1) (2013) 21–30.
[33] S.K. Chen, Simultaneous reduction of NOx and particulate emissions by using multiple injections in a small diesel engine, SAE Trans. (2000) 2127–2136.
[34] K.A. Zahan, M. Kano, Biodiesel production from palm oil, its by-products, and mill effluent: a review, Energies 11 (8) (2018) 2132.
[35] Basavaras B. Patil, S.N. Topannavar, K.M. Akkoli, M.M. Shivashimpi, Sunilkumar S. Kattimani, Experimental investigation to optimize nozzle geometry and compression ratio along with injection pressure on single cylinder DI diesel engine operated with AOME biodiesel, Energy 254 (2022), 124185.
[36] M.M. Shivashimpi, S.A. Alur, N.R. Banapurmath, Exhaust gas recirculation as a NOx reduction technique for modified POME fuelled diesel engine, Int. J. Veh. Struct. Syst. 14 (2) (2022).
[37] R.D. Reitz, Controlling DI diesel engine emissions using multiple injections and EGR, Combust. Sci. Technol. 138 (1–6) (1998) 257–278.
[38] J. Lee, S. Choi, S. Shin, H. Choi, K. Min, Experimental analysis of emission reduction by the split injection strategy using close post injection with a double-row nozzle in heavy EGR conditions, J. Mech. Sci. Technol. 26 (4) (2012) 1265–1274.
[39] A. Jain, A.P. Singh, A.K. Agarwal, Effect of split fuel injection and EGR on NOx and PM emission reduction in a low temperature combustion (LTC) mode diesel engine, Energy 122 (2017) 249–264.
[40] G.R. Kothiwale, K.M. Akkoli, B.M. Doddamani, S.S. Kattimani, Ü. Ağbulut, A. Afzal, A.R. Kaladgi, Z. Said, Impact of injector nozzle diameter and hole number on performance and emission characteristics of CI engine powered by nanoparticles, Int. J. Environ. Sci. Technol. (2022) 1–22.
[41] N.R. Banapurmath, P.G. Tewari, Performance studies of a low heat rejection engine operated on non-volatile vegetable oils with exhaust gas recirculation, Int. J. Sustain. Eng. 2 (4) (2009) 265–274, https://doi.org/10.1080/19397030903215984.

[42] Mahantesh Shivashimpi, Sidramappa Alur, Nagaraj Banapurmath, Uday Kapale, Optimization of multiple injection strategy in modified common rail direct injection diesel engine powered with palm oil methyl ester, Chemistry 7 (1) (2019) 87–99.
[43] Upendra Rajak, Prerana Nashine, Abhishek Dasore, Ramakrishna Balijepalli, Prem Kumar Chaurasiya, Tikendra Nath Verma, Numerical analysis of performance and emission behavior of CI engine fueled with microalgae biodiesel blend, Mater. Today 49 (2022) 301–306. Proceedings.
[44] Abhishek Dasore, Upendra Rajak, Manoj Panchal, V. Nageswara Reddy, Tikendra Nath Verma, Prem Kumar Chaurasiya, Prediction of overall characteristics of a dual fuel CI engine working on low-density ethanol and diesel blends at varying compression ratios, Arabian J. Sci. Eng. (2022) 1–8.